Hindawi
International Journal of Optics
Volume 2021, Article ID 6642261, 5 pages
https://doi.org/10.1155/2021/6642261

Research Article

Investigation on Coaxial Multiwavelength Generation in a CVD Diamond Crystal in the Near-IR Regime

Jingjie Hao,[1,2] Ze Lv,[1,2] Yu Shen ,[1,3] Nan Zong,[1,3] Wei Tu,[1,3] Shenjin Zhang ,[1,3] Yong Bo,[1,3] Qinjun Peng,[1,3] and Zuyan Xu[1,3]

[1]*Key Lab of Solid State Laser, Technical Institute of Physics and Chemistry, Chinese Academy of Sciences, Beijing 100190, China*
[2]*University of Chinese Academy of Sciences, Beijing 100190, China*
[3]*Key Lab of Functional Crystal and Laser Technology, Technical Institute of Physics and Chemistry, Chinese Academy of Sciences, Beijing 100190, China*

Correspondence should be addressed to Yu Shen; shenyu@mail.ipc.ac.cn and Shenjin Zhang; zhangshenjin@163.com

Received 14 November 2020; Revised 5 May 2021; Accepted 17 September 2021; Published 22 October 2021

Academic Editor: Quan Sheng

Optical properties and high-order stimulated Raman scattering (SRS) generation in a homemade CVD diamond crystal with $3 \times 3\,mm^2$ aperture are investigated in this paper. The high order of the Raman laser has been studied theoretically and demonstrated experimentally. By simulating the Stokes components at different pump intensities and the divergence angles, the pump source was well matched with the size of the crystal. Pumped by using a 1064 nm picosecond laser, five coaxial wavelengths were obtained for the first time based on the CVD diamond at 932 nm, 1064 nm, 1240 nm, 1485 nm, and 1851 nm. This work provides a reference for further development of the optical grade diamond crystal with a large aperture.

1. Introduction

As a common approach to achieve multiple-wavelength output, stimulated Raman scattering (SRS) has played an important role in the fields of information storage, multiwavelength communication, and multispectral sensing. Crystals such as vanadates (YVO_4 and $GdVO_4$), tungstates ($BaWO_4$), nitrates ($Ba(NO_3)_2$), and iodates ($LiIO_3$) have been utilized in SRS generation for exploring a wider spectral range [1–4]. At present, the reported Raman lasing spectrum has fulfilled the coverage from infrared and visible to ultraviolet, and the operation mode has also extended from the multilongitudinal mode to single frequency [5, 6].

In addition to the aforementioned traditional Raman crystals, Raman lasers based on diamond have attracted extensive attention in recent years, especially with the rapid development of chemical vapor deposition (CVD) technology. The CVD diamond not only has inherent qualities such as its high hardness, good thermal conductivity, and wide transparent range but also has higher purity and lower defects compared with the natural diamond [7]. At present, the diamond becomes a strong competitor in the field of Raman lasers because of its large Raman frequency shift, high Raman gain coefficient, and extremely high thermal conductivity [7, 8]. As an important starting point to study the Raman properties of diamond, the properties of the first Stokes have been paid much attention under different pump conditions. Jelinek et al. reported a 1632 nm laser, which was pumped by a nanosecond 1339 nm laser [9]. Sabella et al. reported a 1240 nm laser pumped by the 1064 nm nanosecond pulse with an external resonator [10]. With a 1047 nm Nd: YLF pump laser, a continuous wave (CW) at 1217 nm was achieved by Savitski et al. [11]. Granados et al. reported 275.7 nm, which was pumped by a 266 nm picosecond laser obtained by the 4th harmonic of an Nd: YVO_4 laser [12]. For the research on the generation of multiple wavelengths, Kaminskii et al. demonstrated the first experimental detection of one Stokes and three anti-Stokes components by the 1064 nm picosecond laser in 2004 [13]. In 2014, Lux et al. realized the highest order of Stokes in the near-IR regime, and up to three Stokes components were reported [14]. Subsequently, Sabella et al. reported a diamond Raman laser (DRL) with output wavelength tuned from 3.38 to 3.80 μm, which was pumped by an optical parametric oscillator [15]. In addition, due to the beam cleaning effect during the SBS process and the excellent thermal management ability of diamond, DRLs are also used to enhance the brightness of the beam while wavelength conversion. Bai et al. realized 1240 nm first-order and 1485 nm second-order Raman conversion in diamond, generating the brightness enhancement factors up to 12.7 and 6.0, respectively [16, 17].

In this article, the optical properties of a homemade CVD diamond are explored in detail. The basic properties such as surface roughness and transmittance of the samples are tested. The coaxial output of five wavelengths in diamond pumped by a 1064 nm picosecond laser is investigated theoretically and experimentally, among which the order of Stokes is the same as the highest order reported worldwide. The result paves the way for improving the quality of the homemade CVD diamond and utilizing it for Raman laser generation.

2. Optical Properties of the Diamond

In this study, the diamond used is joint designed and grown by Ningbo Institute of Materials Technology and Engineering, CAS. The dimensions of the CVD diamond crystal used are 3 mm × 3 mm × 6 mm with both facets polished and uncoated. It is cut for transmitting along the <110> axial. We have measured the surface roughness and the transmittance in the near-infrared regime, and the corresponding results are shown in Figure 1 and Table 1. It is found that the local surface is extremely unsmooth, and the cutting mark is pervasive. The arithmetic means roughness and the root mean square (RMS) roughness are 3.099 nm and 3.896 nm, respectively. The main reasons for the unsatisfactory surface of the sample are the immature technologies in the process of lapping and polishing. Based on the ratio of transmittance, the attenuation coefficient is calculated to be 0.588 cm^{-1}, which is much higher than the previous report (<0.1 cm^{-1}) [17, 18]. Higher absorption loss will lead to lower conversion efficiency, especially for CW pumped Raman oscillators. However, it is more suitable for short-pulse pumping with high peak power.

3. Theoretical Analyses

In order to obtain high-order Raman scattering simultaneously, a preliminary simulation is conducted. Since the dephasing time of the diamond $T_R \approx 4.2$ ps [13] is comparable to the pulse width of the picosecond pump source we used ($\tau_p \approx 30$ ps), the simulation below is carried out under the transient state regime, which means the Stokes components of the diamond are related to the pump energy $\tau_p I_p$. The distribution of the pump laser in diamond, pump intensity, and divergence angles for different wavelengths are the main factors that need to be taken into consideration. Given that a shaping system containing two lenses will be used to match the pump source to the crystal in the experiment, in the case of a fixed pump radius of 4 mm, we

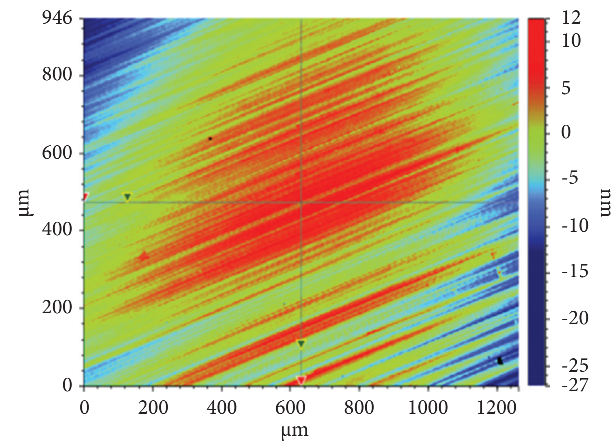

Figure 1: The surface roughness in the near-IR regime.

Table 1: The results of surface roughness and transmittance measurement.

Parameters	Value
Ra (nm)	3.099
Rq (nm)	3.896
Transmittance at 1064 nm	70%
Attenuation coefficient (cm^{-1})	0.588

have simulated the radius of the pump beam in different positions of the crystal by adjusting the distance between the two convex lenses (f300 and f100 are used here) in front of the CVD diamond. And the corresponding results are shown in Figure 2. With the increase of this distance, the pump beam in the crystal diverges first, then becomes nearly parallel, and gradually becomes smaller.

The generation of Stokes components in the CVD diamond is calculated based on the following equations:

$$\begin{aligned} \frac{\partial \mathrm{Ip}}{\partial z} &= -g_R I_p I_{S_1} - \alpha_0 I p, \\ \frac{\partial I_{S_1}}{\partial z} &= g_{R_1} I_{S_1}\left(I_p - I_{S_2}\right) - \alpha_0 I_{S_1}, \\ \frac{\partial I_{Sn}}{\partial z} &= g_{Rn} I_{Sn}\left(I_{Sn} - I_{Sn+1}\right) - \alpha_0 I_{Sn}, \end{aligned} \tag{1}$$

where I_{Sn} ($n = 1$, 2, 3, and 4) and I_p are the intensity of each order of Stokes and the pump source. z is the transmitting distance in the Raman crystal. g_{Ri} is the Raman gain coefficient for the ith Stokes component, and it is derived from $g_{Ri} = g_R \omega_{Si}/\omega_p$, where g_R is the Raman gain coefficient and ω_{Si} and ω_p are the frequency of the pump and ith Stokes, respectively. The Stokes intensity will be enlarged as it propagates the distance z through the Raman gain medium, and the gain coefficient g_R is related to the differential scattering cross section [19]. The gain coefficient of diamond reported is 15 cm/GW at 1 μm band [20]. Therefore, g_{R1}, g_{R2}, and g_{R3} in simulation are 12.87 cm/GW, 10.75 cm/GW, and 8.62 cm/GW, respectively. α_0 is the extinction coefficient, which is set as 0.1 cm^{-1} and 0.588 cm^{-1}, respectively. Figure 3 indicates that the pump intensity has a

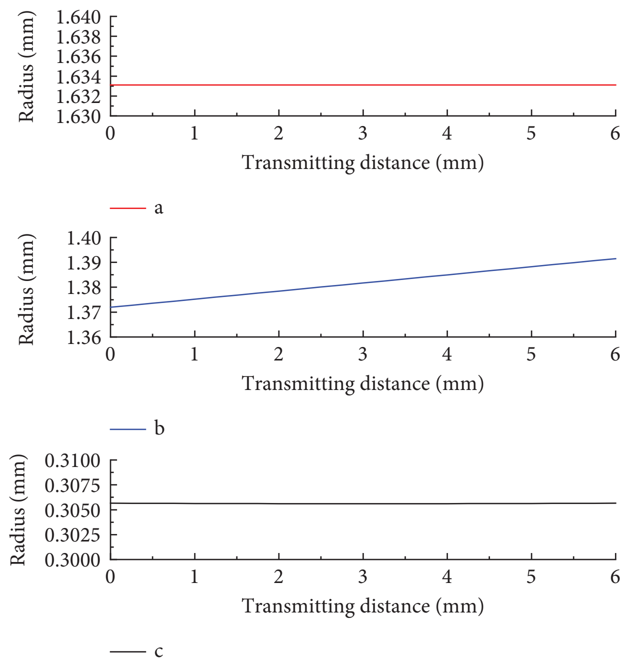

Figure 2: The radius of the pump beam in different positions of the crystal. And the distance between the two convex lenses (f300 and f100) is 380 mm (b), 400 mm (a), and 410 mm (c), respectively.

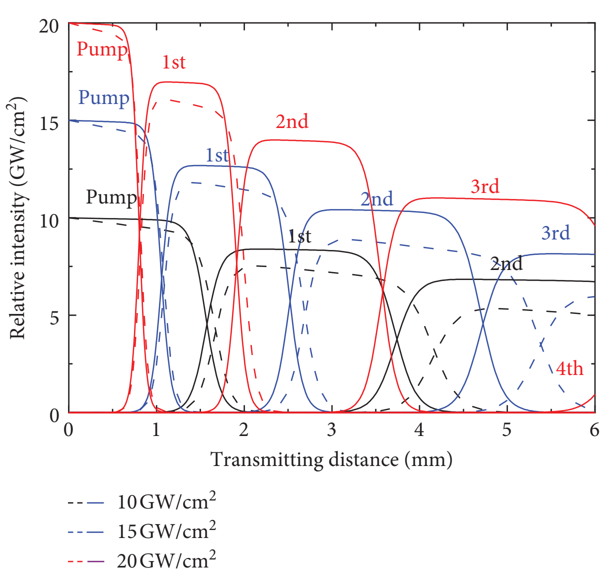

Figure 3: The relative intensity of each order of Stokes components with respect to the transmitting distance in the CVD diamond crystal under the pump intensity of 10 GW/cm^2 (the black lines), 15 GW/cm^2 (the blue lines), and 20 GW/cm^2 (the red lines). The extinction coefficients for solid lines and dashed lines are 0.1 cm^{-1} and 0.588 cm^{-1}, respectively.

significant influence on the generation of the high-order Stokes. And the intensities of the Stokes components will be reduced if the extinction coefficient of the sample is too large.

Then, the divergence angles of four Stokes components are calculated to be 2.294°, 5.511°, 8.257°, and 10.540°, using the phase-matching condition and Sellmeier equation. Based on the theoretical analysis above, to make sure that all the generated Stokes can be detected by the spectrometer rather than be blocked by the sidewall of the crystal, the radius of pump light in the crystal should not be larger than 1.1 mm under the pump energy intensity of 20 GW/cm^2. The condition poses no challenge to implementation, for example, by slight adjustment on the distance between the two convex lenses around 400 mm.

4. Experimental Setup and Results

The schematic of the experiment is shown in Figure 4. A diode-pumped mode-locked Nd: YVO_4/YAG 1064 nm laser (PL2251A-10-SH, Ekspla Corporation) is applied as the pump source to the Raman generator. The pump pulse duration and repetition rate are 30 ps and 10 Hz, respectively. The diameter of the pump beam is 8 mm. And the beam quality factor M^2 is 1.5. M is a 45° highly reflecting mirror for the pump laser. An optical beam-shaping system, which comprises two convex lenses with 300 mm and 100 mm focal lengths, is used to decrease the pump beam diameter. Then, an aperture is applied with a diameter of 1.1 mm to make the pump beam match with the crystal as well as filter the stray light. The diamond is mounted onto a copper holder for heat spreading. To control the temperature of the sample, circuit cooling water was used with a temperature of 18°C. The spectrum of the output laser is detected by using a commercial spectrometer (NIRQuest-256, Ocean Insight), with wavelength ranging from 850 to 2500 nm and resolution ~9.5 nm.

With the experimental setup, the SRS is generated by focusing the fundamental laser beam into the diamond crystal. The first Stokes radiation is measured to be 1240 nm

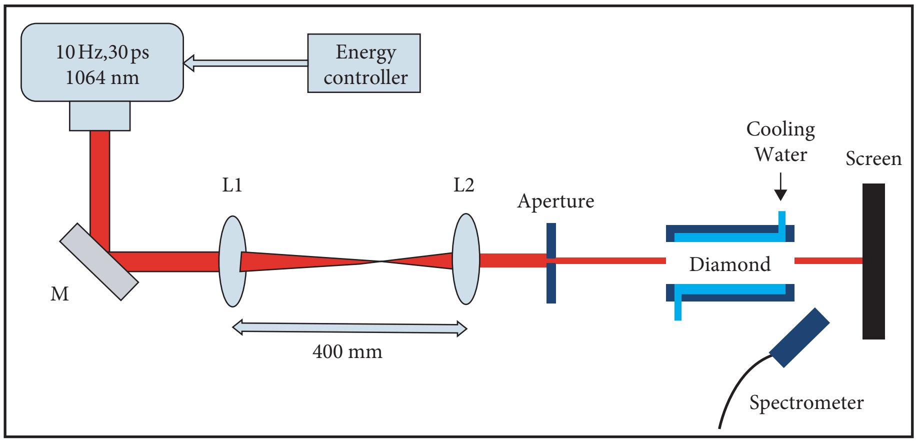

FIGURE 4: Experimental schematic for SRS in the CVD diamond crystal.

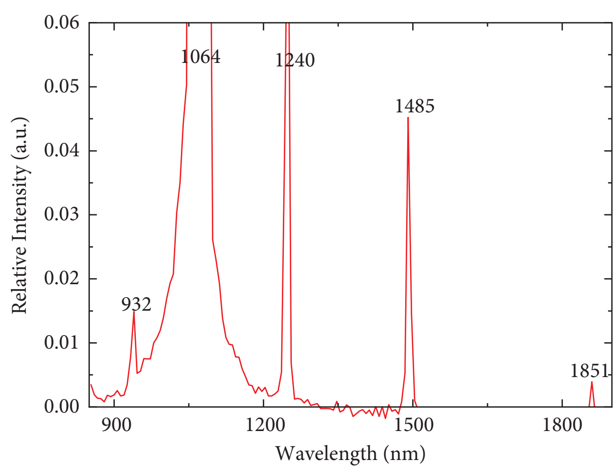

FIGURE 5: SRS spectrum of the diamond pumped by a 1064 nm picosecond laser.

TABLE 2: Spectral composition of Stokes and anti-Stokes generated in the CVD diamond crystal under the pump of the picosecond 1064 nm laser.

λ_p (nm)	Stokes and anti-Stokes components		
	Wavelength (nm)	$\chi(3)$ lasing component	Threshold (GW/cm^2)
1064	932	AS_{t1}	18.6
	1064	λ_p	—
	1240	S_{t1}	8.5
	1485	S_{t2}	11.8
	1851	S_{t3}	18.6

when reaching the SRS threshold. With the increase of the pump power, three orders of Stokes and one order of anti-Stokes components are observed in succession. The output spectrum was measured under the maximum pump intensity of 18.6 GW/cm^2 as shown in Figure 5. The corresponding thresholds are summarized in Table 2. The simulated results are nearly the same as the characteristics of the output spectrum, which could be applied as a feasible reference for the simulation of the Raman generator. However, a dot (optical breakdown) in the crystal was found during the detection process. Thus, the damage threshold for the CVD diamond is close to 18.6 GW/cm^2, which means that this sample is qualified for operating at high power.

5. Conclusion

In summary, the optical quality of a homemade CVD diamond is evaluated by testing and experimental verification. Pump by using a picosecond laser, output with five spectral components (including three Stokes and one anti-Stokes) is achieved. According to the previous reports, the cross section of commonly used optical grade diamond crystals is about $4 \times 1.2\,mm^2$ [16, 21]; however, here, a $3 \times 3\,mm^2$ diamond based on our growth technology is used for SRS generation. The optical test results show that there is still room for improving the ratio of transmittance and the precision of postprocessing of the CVD diamond. Next, further improvement of diamond purity and CVD growth process will be carried out to obtain a larger-diameter optical grade diamond crystal, which will be of great value to improve the output power of DRLs as well as Brillouin lasers in the future [8, 22, 23].

Data Availability

No data were used to support this study.

Disclosure

Jingjie Hao and Ze Lv are the co-first authors.

Conflicts of Interest

The authors declare that they have no conflicts of interest.

Authors' Contributions

Jingjie Hao and Ze Lv contributed equally to this work.

Acknowledgments

This research was supported by the grant of the Key Laboratory Foundation by the Technical Institute of Physics and Chemistry, CAS. The authors also acknowledge the support (CVD diamond growth) from Ningbo Institute of Materials Technology and Engineering, CAS.

References

[1] A. A. Kaminskii, K. Ueda, H. J. Eichler et al., "Tetragonal vanadates YVO_4 and $GdVO_4$–new efficient χ (3)-materials for Raman lasers," *Optics Communications*, vol. 194, no. 1-3, pp. 201–206, 2001.

[2] P. Černý, P. G. Zverev, H. Jelınková, and T. T. Basiev, "Efficient Raman shifting of picosecond pulses using $BaWO_4$ crystal," *Optics communications*, vol. 177, no. 1–6, pp. 397–404, 2000.

[3] P. G. Zverev, J. T. Murray, R. C. Powell, R. J. Reeves, and T. T. Basiev, "Stimulated Raman scattering of picosecond pulses in barium nitrate crystals," *Optics Communications*, vol. 97, no. 1-2, pp. 59–64, 1993.

[4] H. M. Pask and J. A. Piper, "Diode-pumped LiIO3 intracavity Raman lasers," *IEEE Journal of Quantum Electronics*, vol. 36, no. 8, pp. 949–955, 2000.

[5] Q. Sheng, R. Li, A. J. Lee, D. J. Spence, and H. M. Pask, "A single-frequency intracavity Raman laser," *Optics Express*, vol. 27, no. 6, pp. 8540–8553, 2019.

[6] Q. Sheng, A. Lee, D. Spence, and H. Pask, "Wavelength tuning and power enhancement of an intracavity Nd:GdVO4-BaWO4 Raman laser using an etalon," *Optics Express*, vol. 26, no. 24, pp. 32145–32155, 2018.

[7] R. Mildren and J. Rabeau, *Optical Engineering of Diamond*, John Wiley & Sons, Hoboken, NJ, USA, 2013.

[8] R. J. Williams, O. Kitzler, Z. Bai et al., "High power diamond Raman lasers," *IEEE Journal of Selected Topics in Quantum Electronics*, vol. 24, no. 5, Article ID 1602214, 2018.

[9] M. Jelinek, O. Kitzler, H. Jelinkova, J. Sulc, M. Nemec, and V. Kubecek, "CVD-diamond external cavity Raman laser operating at 1632 nm," in *Proceedings of the Quantum Electronics Conference & Lasers & Electro-Optics*, Sydney, Australia, September 2011.

[10] A. Sabella, J. A. Piper, and R. P. Mildren, "1240 nm diamond Raman laser operating near the quantum limit," *Optics Letters*, vol. 35, no. 23, pp. 3874–3876, 2010.

[11] V. G. Savitski, I. Friel, J. E. Hastie, M. D. Dawson, D. Burns, and A. J. Kemp, "Characterization of single-crystal synthetic diamond for multi-watt continuous-wave Raman lasers," *IEEE Journal of Quantum Electronics*, vol. 48, no. 3, pp. 328–337, 2011.

[12] E. Granados, D. J. Spence, and R. P. Mildren, "Deep ultraviolet diamond Raman laser," *Optics Express*, vol. 19, no. 11, pp. 10857–10863, 2011.

[13] A. A. Kaminskii, V. G. Ralchenko, and V. I. Konov, "Observation of stimulated Raman scattering in CVD-diamond," *Journal of Experimental and Theoretical Physics Letters*, vol. 80, no. 4, pp. 267–270, 2004.

[14] O. Lux, V. G. Ralchenko, A. P. Bolshakov et al., "Multi-octave frequency comb generation by χ (3)-nonlinear optical processes in CVD diamond at low temperatures," *Laser Physics Letters*, vol. 11, no. 8, Article ID 086101, 2014.

[15] A. Sabella, J. A. Piper, and R. P. Mildren, "Diamond Raman laser with continuously tunable output from 338 to 380 μm," *Optics Letters*, vol. 39, no. 13, pp. 4037–4040, 2014.

[16] Z. Bai, R. J. Williams, H. Jasbeer et al., "Large brightness enhancement for quasi-continuous beams by diamond Raman laser conversion," *Optics Letters*, vol. 43, no. 3, pp. 563–566, 2018.

[17] Z. Bai, R. J. Williams, O. Kitzler, S. Sarang, D. J. Spence, and R. P. Mildren, "302 W quasi-continuous cascaded diamond Raman laser at 15 microns with large brightness enhancement," *Optics Express*, vol. 26, no. 16, pp. 19797–19803, 2018.

[18] X. Yang, O. Kitzler, D. J. Spence, Z. Bai, Y. Feng, and R. P. Mildren, "Diamond sodium guide star laser," *Optics Letters*, vol. 45, no. 7, pp. 1898–1901, 2020.

[19] R. L. Sutherland, *Handbook of Nonlinear Optics*, CRC Press, Boca Raton, FL, USA, 2003.

[20] I. Friel, S. L. Geoghegan, D. J. Twitchen, and G. Scarsbrook, "Development of high quality single crystal diamond for novel laser applications," *Proceedings of SPIE—The International Society for Optical Engineering*, vol. 7838, 2010.

[21] R. J. Williams, J. Nold, M. Strecker et al., "Efficient Raman frequency conversion of high-power fiber lasers in diamond," *Laser & Photonics Reviews*, vol. 9, no. 4, pp. 405–411, 2015.

[22] Z. Bai, R. J. Williams, O. Kitzler et al., "Diamond Brillouin laser in the visible," *APL Photonics*, vol. 5, no. 3, Article ID 031301, 2020.

[23] S. Antipov, A. Sabella, R. J. Williams, O. Kitzler, D. J. Spence, and R. P. Mildren, "12 kW quasi-steady-state diamond Raman laser pumped by an $M^2 = 15$ beam," *Optics Letters*, vol. 44, no. 10, pp. 2506–2509, 2019.